

# MICROSTRUCTURAL ORIGIN OF THE DIELECTRIC BREAKDOWN STRENGTH IN ALUMINA: A STUDY BY POSITRON LIFETIME SPECTROSCOPY

Abderrahmane SI AHMED<sup>1</sup>, Jerzy KANSY<sup>1,2</sup>, Kamel ZARBOUT<sup>1</sup>, Gérard MOYA<sup>1</sup>, and Dominique GÆURIOT<sup>3</sup>

<sup>1</sup> L2MP, U.M.R./CNRS 6137, Faculté des Sciences de St. Jérôme, F 13397 Marseille, France

<sup>2</sup> Inst. of Physics and Chem. of Metals, Silesian University, Bankowa 12, Pl 40-007 Katowice, Poland

<sup>3</sup> Ecole Nationale Supérieure des Mines de Saint-Etienne, F 42023 St-Etienne, France

## Abstract

The dielectric breakdown strengths of two series of sintered alumina samples (of low and high impurity content, with Si being the dominant element) and single crystals are compared with positron lifetime measurements. It is found that the breakdown strength increases linearly with increasing concentration of positron traps at grain boundaries. These traps are likely clusters containing negatively charged cationic vacancies, which are induced by silicon dissolution into  $Al_2O_3$ . Therefore, the improvement of the breakdown strength can be traced to silicon segregation at grain boundaries. A solubility of Si in  $Al_2O_3$ , achieved during the firing schedule of the sintering process, and which does not take into account enhanced solubility caused by mutual compensation of Si with other lower valence foreign cations such as Ca and Mg, is estimated at 120 ppm.

## 1. Introduction

Positron Annihilation Lifetime Spectroscopy (PALS) is sensitive to vacancy-like defects in materials [1]. In oxides, the dissolution of foreign cations, greater or lesser in valence than the host cation, requires that charged point defects be created in order to preserve electrical neutrality. Neutral and negatively charged vacancies (or vacancy clusters) act as positron traps. In  $Al_2O_3$ , only the cations greater in valence than Al, such as Si, can induce negatively charged vacancies, namely the cationic vacancies  $V_{Al}'''$  [2,3]. In addition, the defect structure achieved during the firing schedule of the sintering process comprises, among other defects, isolated  $V_{Al}'''$  as well as neutral and negatively charged defect complexes containing cationic vacancies [3,4].

In previous work [4, 5], PALS measurements were carried out in two series of sintered  $Al_2O_3$  samples. In both materials, Si was the dominant impurity (i.e., 90 ppm and 1500 ppm). Two lifetime components of 137 ps and 400 ps were resolved for both series, which can be interpreted as an indication that the natures of positron traps are identical in the two materials. The shorter lifetime was assigned to  $V_{Al}'''$  located within the grain and the other to grain boundaries clusters (i.e., likely  $V_{Al}'''$  associated with segregated impurities [4]). The dielectric breakdown strengths of the same sintered and of single crystals have also been reported [6].

The purpose of this work is to improve the understanding of the microstructural origin of the dielectric breakdown by calling for the nature and localisation of defects that are provided by PALS measurements. An earlier attempt to establish a relation between the breakdown strength and PALS measurements has been suggested [6]. Here, the *two state trapping model*, which considers only one trapping process, was used. In the present work, the results derived from a more complete description (i.e., *the three state trapping model* [7]) are utilised. This

description allows an access to positron trapping in defects located within the grain and at gain boundaries.

## 2. Materials preparation and experimental

### 2.1 Materials characteristics and preparation

The material referred below as doped samples contained SiO<sub>2</sub> (1497 ppm), MgO (723 ppm), CaO (686 ppm), Fe<sub>2</sub>O<sub>3</sub> (415 ppm) and Na<sub>2</sub>O (404 ppm). The other one considered as pure contained SiO<sub>2</sub> (90 ppm) Na<sub>2</sub>O (40 ppm) and background impurities (of total amount near 20 ppm). Sintering was performed in air and the different grain diameters were reached by controlling the firing schedule [6].

### 2.2 Breakdown strength determination

The experimental set up and the measurement procedure were described in Ref [6]. The breakdown strength  $E_c$  as a function of specific surface of grain boundaries ( $s_{GB}$ ) are plotted in Fig. 1. The specific surface is estimated by assuming grains of spherical shapes, i.e.,  $s_{GB} = 3/R$  where  $R$  is the mean radius of grains. For pure sample,  $E_c$  seems to be constant at value about 15.2 kV/mm whereas for doped ones a linear dependence  $E_c = 0.454 s_{GB} + 12.16$  kV/mm is observed. The value of the breakdown strength of a single crystal (12.3 kV/mm) is also given, which evidently corresponds to an infinite grain radius.

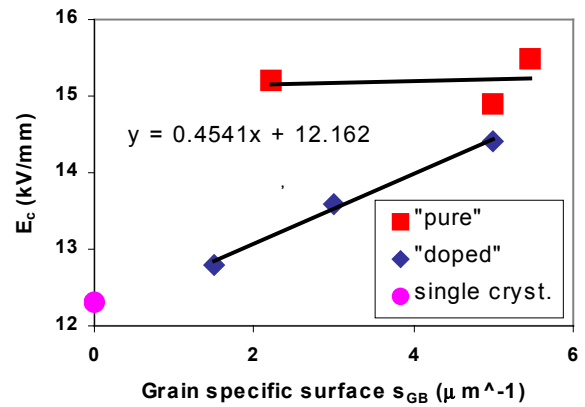


Fig 1. Breakdown strength versus specific surface of grains in alumina samples of different impurity contents.

### 2.3 Positron lifetime measurements : analysis and results

For the PALS experiments, the same single crystal and doped samples were taken as in the breakdown strength measurements. However, in the case of pure material, two other samples were used. These samples have the same impurity contents as those of Fig 1, but differ by their grain size [4]. The positron lifetime spectra were recorded at room temperature using a conventional fast-fast coincidence system. The spectra were measured in 2000 channels (calibration 27 ps/channel and FWHM of 270 ps) and collected about  $6 \times 10^6$  counts. They were analysed via a *LT v.9 program* [8], in which the *three-state trapping model* [8] was introduced into the source code. The three states refer to different locations of positron annihilation (i.e., in the bulk material, in vacancies within the grains and in defects at grain boundaries). In the case of doped samples, the first state (annihilations in the bulk) turned out to be negligible. In single crystal, the third process (annihilation at grain

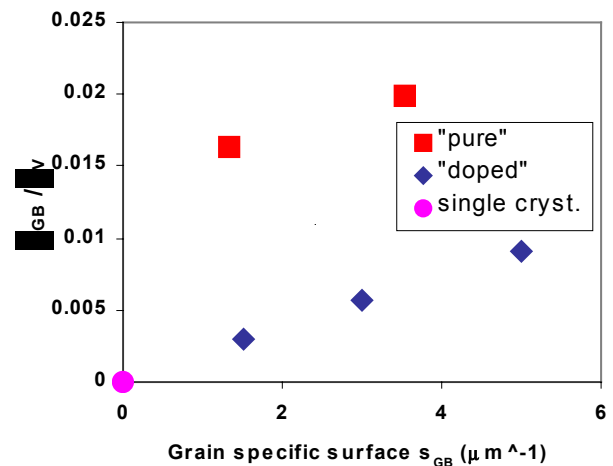


Fig 2. The ratio of positron trapping rates  $\kappa_{GB} / \kappa_V$  into defects at grain boundaries and into vacancies inside grains versus specific surface of grains..

boundaries) is considered equal to zero as there are no grain boundaries. The details of the experiments and their analyses have been described in our previous works [4, 5]. In Fig 2, the ratio  $\kappa_{GB} / \kappa_V$  (where  $\kappa_{GB}$  and  $\kappa_V$  are respectively the positron trapping rates in defects at grain boundaries and in defects within the grain) is plotted as a function of  $s_{GB}$ . Only these PALS spectrum parameters are of interest for the scope of this paper.

### 3. Discussion

From the comparison of Fig 1 and Fig 2, one can observe that the dependences of  $E_c$  and  $\kappa_{GB} / \kappa_V$  on  $s_{GB}$  are quite similar. This suggests a correlation between  $E_c$  and the ratio  $\kappa_{GB} / \kappa_V$ . According to the trapping model, this ratio is proportional to  $c_{GB} / c_V$ , where  $c_{GB}$  and  $c_V$  express concentrations of positron traps within the grains and at grain boundaries. The proportionality factor is expected to be of order of unit. For a given type of samples,  $c_V$  has almost a constant value, i.e. independent of the grain size [4]. Consequently, the variations of the ratio  $\kappa_{GB} / \kappa_V$  reflect, in fact, changes of the concentration of positron traps,  $c_{GB}$ , at grain boundaries. To determine the changes of  $c_{GB} = \text{const} \times c_V \kappa_{GB} / \kappa_V$  the concentration  $c_V$  within the grains in pure and doped samples must be known.

For pure samples,  $c_V$  can be estimated, with some assurance, from the Si content, at about 28 ppm [4]. However, in the case of doped samples,  $c_V$  cannot be evaluated on the basis of impurity content, because it is so high that  $c_V$  achieves its ultimate value, which is determined by the solubility of Si. Assuming that the correlation between  $E_c$  and  $c_{GB}$  is the same for pure and doped samples, one could estimate the unknown value  $c_V$  for doped samples by fitting a straight line to all of the experimental points in the plot  $E_c$  against  $c_{GB} = \text{const} \times c_V \kappa_{GB} / \kappa_V$  (Fig 3). The best fit can be obtained if  $c_V$  in doped samples is 40 ppm. Taking into account that a vacancy is induced by the dissolution of three Si atoms [4], one can estimate the “*apparent*” solubility limit of Si at 120 ppm (here it must be reminded that Si is the only foreign element whose dissolution can give birth to negatively charged cationic vacancies  $V_{Al}'''$  and hence to positron traps [2, 3]). This value is lower than the solubility limit reported in Ref [9] and [10] under sintering conditions close to ours. There, Si level in the range 200-300 ppm was found just sufficient for the formation of glassy grain boundary films. We have to acknowledge that PALS cannot reflect the actual solubility limit of Si in the doped samples. Indeed, some fraction of silicon could be prevented from inducing  $V_{Al}'''$ , due to possible mutual compensation of Si with impurities of lower valence, such as Ca and Mg [10], which are present in substantial amount in the doped samples. Therefore, the departure of this “*apparent*” solubility limit (120ppm) from the actual solubility one (200-300 ppm) could be seen as an assessment of the mutual compensation effects, i.e., enhancement of Si solubility in  $Al_2O_3$  induced by Ca and Mg).

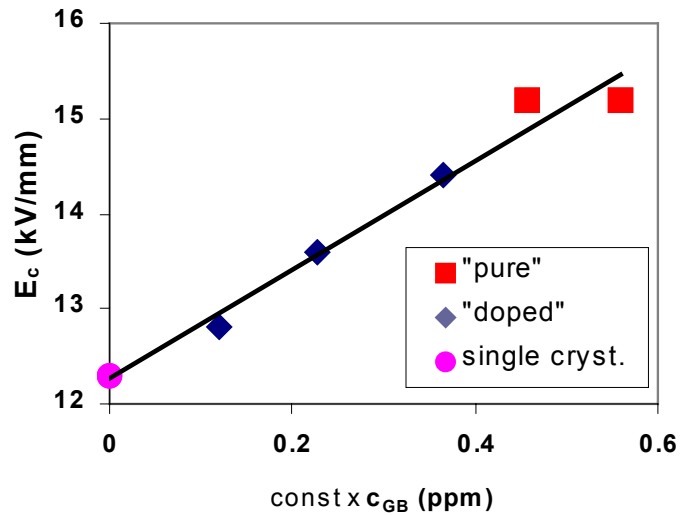


Fig 3. Breakdown strength as a function of defect concentration at grain boundaries. The straight line represents the best fit to the points (see text).

The correlation which emerges from Fig 3 indicates that the breakdown strength is improved by the existence of grain boundaries. However, it illustrates that such an improvement can be furthermore traced to the concentration of positron traps at grain boundaries. Since the positron traps are induced by Si dissolution into  $\text{Al}_2\text{O}_3$ , the breakdown strength is also sensitive to silicon segregation. Such a correlation appears as a signature of the effect of the microstructural development (generated during the sintering process) on a macroscopic property, i.e. the dielectric breakdown strength. However, a relevant question arises (i.e., Why the concentration of positron traps seems higher in the pure samples than in the doped ones as it appears in Fig 3 ?). Here again, mutual compensation effects could be responsible. Furthermore, preferential segregation of other foreign elements, and in particular of Ca which has the highest enrichment ratio [11], could reduce the concentration of Si at grain boundaries. Finally, one cannot exclude the formation of glassy grain boundary films. In any case, further clarification of this question requires investigations using several series of materials of well defined impurity contents. To this end, this work provides a framework, which can also be geared to the optimisation of the dielectric properties of sintered alumina.

#### 4. References

- [1] P. Hautojärvi (ed.), Positron in Solids Springer-Verlag, Berlin (1979)
- [2] R.W. Grimes: J. Am. Ceram. Soc. Vol. 77 (1994), p. 378
- [3] K.P.D. Lagerlöf and R.W. Grimes: Acta mater. Vol. 46 (1998), p. 5689
- [4] G. Moya, J. Kansy, A. Si Ahmed, J. Liebault, F. Moya and D. Gœuriot: Phys. Stat. Sol. (a) Vol. 198 (2003), p. 215
- [5] A. Si Ahmed, J. Kansy, K. Zarbout, G. Moya and D. Gœuriot : Mater. Sci. Forum Vol. 445-446 (2004), p.177
- [6] J. Liebault, A. Si Ahmed, J. Kansy, D. Gœuriot and G. Moya, 4<sup>th</sup> Internat. Conf. On Electric Charges in Non-Conductive Materials, Tours (F), 1-6 July 2001 : Le Vide – Science , Technique et Applications (2001), p.165
- [7] R. Krause-Rehberg, H.S. Leipner, Positron Annihilation in Semi-conductors, Springer-Verlag, Berlin (1999)
- [8] J. Kansy, Nucl. Instr. & Meth. A 347 (1996), p. 235
- [9] S.I. Bae, S. Baik, J. Am. Ceram. Soc., 76 (1993), p. 1065
- [10] K.L. Gavrilov, S.J. Bennison, K.R. Mikeska , J.M. Chabala, R. Levy-Setti, J. Am. Ceram. Soc., 82, (1999), p. 1001
- [11] E. Dörre and H. Hübner : Alumina, Springer- Verlag, Berlin (1979)